CellPress

Developmental Cell
Article

Cell Intrinsic Modulation of Wnt Signaling Controls Neuroblast Migration in *C. elegans*

Remco A. Mentink,[1] Teije C. Middelkoop,[1] Lorenzo Rella,[1] Ni Ji,[2,3] Chung Yin Tang,[1] Marco C. Betist,[1] Alexander van Oudenaarden,[1,2] and Hendrik C. Korswagen[1,*]

[1]Hubrecht Institute, Royal Netherlands Academy of Arts and Sciences and University Medical Center Utrecht, Uppsalalaan 8, 3584 CT Utrecht, the Netherlands

[2]Department of Physics and Department of Biology, Massachusetts Institute of Technology, 77 Massachusetts Avenue, Cambridge, MA 02139, USA

[3]Department of Brain and Cognitive Sciences, Massachusetts Institute of Technology, 77 Massachusetts Avenue, Cambridge, MA 02139, USA

*Correspondence: r.korswagen@hubrecht.eu

http://dx.doi.org/10.1016/j.devcel.2014.08.008

SUMMARY

Members of the Wnt family of secreted signaling proteins are key regulators of cell migration and axon guidance. In the nematode *C. elegans*, the migration of the QR neuroblast descendants requires multiple Wnt ligands and receptors. We found that the migration of the QR descendants is divided into three sequential phases that are each mediated by a distinct Wnt signaling mechanism. Importantly, the transition from the first to the second phase, which is the main determinant of the final position of the QR descendants along the anteroposterior body axis, is mediated through a cell-autonomous process in which the time-dependent expression of a Wnt receptor turns on the canonical Wnt/β-catenin signaling response that is required to terminate long-range anterior migration. Our results show that, in addition to direct guidance of cell migration by Wnt morphogenic gradients, cell migration can also be controlled indirectly through cell-intrinsic modulation of Wnt signaling responses.

INTRODUCTION

Morphogens such as Wnt proteins play a central role in embryonic patterning by providing positional information to cells in developing tissues. In recent years, it has become clear that such morphogenic gradients also contribute to the guidance of migrating cells and axons in the developing nervous system (Zou and Lyuksyutova, 2007). In the mammalian spinal cord, for example, Wnt gradients control the migration of commissural axons (Liu et al., 2005; Lyuksyutova et al., 2003), and in *C. elegans*, a gradient of the Wnt protein EGL-20 acts as a repulsive guidance cue in the migration of the hermaphrodite-specific neurons (Pan et al., 2006). In addition to acting as direct repulsive or attractive guidance signals, Wnt proteins can also function as permissive factors that enable cells to respond to other guidance cues (Whangbo and Kenyon, 1999; Witze et al., 2008). How migrating cells and growth cones interpret information from Wnt ligands to adopt a specific migratory response is, however, still largely unknown.

Wnt proteins can trigger different signaling cascades in responding cells (Angers and Moon, 2009). In canonical Wnt signaling, binding of Wnt to the receptors Frizzled and Lrp6 leads to stabilization of the cytoplasmic protein β-catenin, which in turn interacts with members of the TCF family of transcription factors to coactivate the expression of specific sets of target genes (Clevers and Nusse, 2012). Wnt can also signal independently of β-catenin through distinct noncanonical Wnt pathways, including a pathway that depends on the receptor tyrosine kinase Ror2 (Green et al., 2008) and a pathway that requires the planar cell polarity (PCP) components Van Gogh (Vangl) and Prickle (Pk) (Wallingford, 2012).

Studies on the role of Wnt signaling in cell and axon migration have been hampered by the complexity of the vertebrate embryo and the multitude of Wnt ligands and receptors that are present in the vertebrate genome. The nematode *C. elegans* offers a more tractable system, with only 5 Wnt ligands, 4 Frizzled receptors, and single orthologs of Ror2, Vangl, and Pk that control the migration and polarity of defined cells and axons (Sawa and Korswagen, 2013). Among the cells that migrate in response to Wnt signaling is the QR neuroblast and its descendants (Figure 1A). During the first stage of larval development, the QR lineage generates a specific set of descendants: an anterior daughter cell (QR.a) that divides once to generate an apoptotic cell and a cell (QR.ap) that differentiates into a chemosensory neuron, and a posterior daughter cell (QR.p) that divides twice to generate an apoptotic cell and two cells (QR.paa and QR.pap) that differentiate into a mechanosensory neuron and an interneuron, respectively (Sulston and Horvitz, 1977). Throughout this process, each QR neuroblast descendant migrates to a highly stereotypic position along the anteroposterior body axis. Previous studies have shown that the migration of QR.p and its descendants (abbreviated as QR descendants unless indicated otherwise) requires multiple Wnt ligands and receptors (Harterink et al., 2011; Kim and Forrester, 2003; Zinovyeva and Forrester, 2005; Zinovyeva et al., 2008). These observations raise the question how the QR descendants integrate this complex Wnt signaling information to migrate to their precisely defined final positions.

Here, we show that the migration of QR descendants can be divided into three sequential phases, each of which is controlled

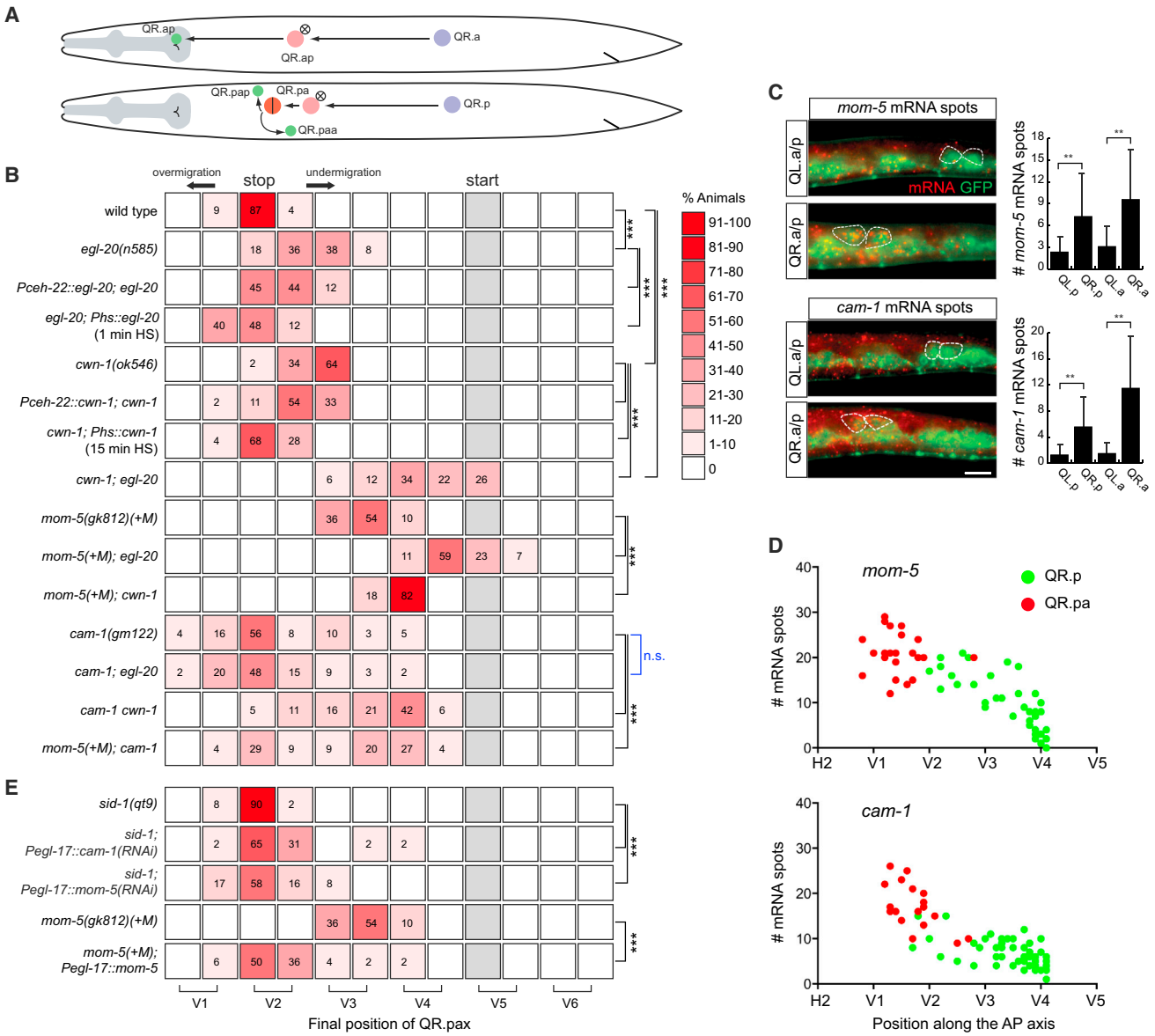

Figure 1. *mom-5*/Frizzled and *cam-1*/Ror2 Act in Parallel Genetic Pathways to Control the Anterior Migration of the QR Descendants

(A) Schematic overview of the anterior migration of QR.a and QR.p and their descendants. Apoptotic cells are indicated as white cells with a cross, while the final QR descendants are indicated in green. The final position of QR.pa division is indicated in red.

(B and E) Average position of the QR descendants QR.pap and QR.paa with respect to the seam cells V1.a to V6.p (lower brackets indicate Vn.a [left] and Vn.p [right] daughters of Vn cells). Values listed are percentiles of the total number of cells scored, n > 50 for all genotypes. A color (red) coded heatmap represents the range of percentile values. The *hsp16.2* HS promoter was used to drive ubiquitous expression of *egl-20* and *cwn-1*, and the time of HS is indicated. The *ceh-22* promoter was used to drive anterior expression of *egl-20* and *cwn-1* in the pharynx (Okkema and Fire, 1994). Q lineage specific RNAi was performed by expressing *cam-1* or *mom-5* dsRNA using the *egl-17* promoter (Burdine et al., 1998) in the RNAi spreading defective mutant *sid-1(qt9)* (Winston et al., 2002). Statistical significance was calculated using Fisher's exact test (***p < 0.0001).

(C) Single-molecule mRNA FISH of *cam-1* and *mom-5* mRNA (red). The Q neuroblasts (outlined with dotted line) and seam cells are labeled with GFP (*hels63*). Quantification of mRNA spots is indicated as mean ± SD (n > 30). Statistical significance was calculated using an unpaired t test (**p < 0.001).

(D) *cam-1* and *mom-5* transcription dynamics in single QR.p (green) and QR.pa (red) neuroblast daughter cells as measured in wild-type animals (n > 60 for both mRNA species). The number of mRNA spots per cell is plotted against the cell position with respect to the seam cells H2 to V5. See also Figure S1.

by a distinct Wnt signaling mechanism. First, anterior migration is mediated through parallel-acting MOM-5/Frizzled- and CAM-1/Ror2-dependent noncanonical Wnt pathways. Second, once QR.pa reaches its final position, anterior migration is stopped by activation of canonical Wnt/β-catenin signaling. Finally, the short-range migration of QR.paa and QR.pap to their specific anteroposterior and dorsoventral positions requires the PCP pathway components VANG-1/Vangl and PRKL-1/Pk. Importantly, we found that Wnt ligands do not act instructively in this process. Instead, our results show that the final position of

QR.pa along the anteroposterior body axis is determined through a cell-intrinsic timing mechanism that turns on canonical Wnt/β-catenin signaling by upregulating the expression of the Wnt receptor *mig-1*. Our results are consistent with a model in which time-dependent switching between Wnt signaling pathways rather than positional information from Wnt ligands controls the highly stereotypic migration of QR.p and its descendants.

RESULTS

The Parallel Acting Wnt Ligands EGL-20 and CWN-1 Do Not Provide Positional Information to the Migrating QR.p Descendants

Mutations in different Wnt ligand and receptor genes have been shown to interfere with the anterior migration of the QR descendants (Harris et al., 1996; Whangbo and Kenyon, 1999; Zinovyeva and Forrester, 2005; Zinovyeva et al., 2008). Using the final anterior position of QR.paa and QR.pap (abbreviated as QR.pax) as a measure of total migration distance, we confirmed that the QR.pax localize at more posterior positions in *egl-20* and *cwn-1* Wnt null mutants (Figure 1B). This defect was strongly enhanced in *cwn-1*; *egl-20* double mutants, indicating that the two Wnt ligands act in parallel to control anterior migration of the QR descendants (Zinovyeva et al., 2008). Mutation of the Wnt gene *cwn-2* did not affect QR.pax localization but enhanced the undermigration phenotype of *egl-20* and weakly of *cwn-1*, consistent with a minor role of *cwn-2* in the migration process (Figure S1A available online).

egl-20 is expressed by a group of cells in the tail region and forms a posterior to anterior concentration gradient that acts instructively in guiding the migration of the hermaphrodite-specific neurons (Coudreuse et al., 2006; Pan et al., 2006; Whangbo and Kenyon, 1999). Previous studies have indicated that this gradient does not function as a directional guidance signal in QR descendant migration (Whangbo and Kenyon, 1999). Consistently, we found that reversal of the EGL-20 concentration gradient, by *ceh-22* promoter directed expression of *egl-20* in the pharynx (Okkema and Fire, 1994), significantly rescues the QR.pax undermigration phenotype of *egl-20* mutants (Figure 1B). However, when *egl-20* was ubiquitously overexpressed using a heat inducible promoter, the QR.pax migrated beyond their wild-type positions (Figure 1B) (Whangbo and Kenyon, 1999), indicating that EGL-20 can promote the migration of the QR descendants when present at elevated levels.

cwn-1 is also expressed in the posterior, but in a broader region than *egl-20* (Harterink et al., 2011; Pan et al., 2006). To investigate whether CWN-1 functions as an instructive guidance signal, we tested if uniform expression of *cwn-1* restores the normal anterior migration of the QR descendants in a *cwn-1* null mutant background. As shown in Figure 1B, heat-shock (HS) promoter directed expression of *cwn-1* rescued the undermigration phenotype of *cwn-1(ok546)*. Furthermore, expression of *cwn-1* in the pharynx also significantly rescued QR.pax migration in the *cwn-1* null mutant background. However, in contrast to *egl-20*, overexpression of *cwn-1* did not induce overmigration of the QR.pax. These results support the notion that morphogenic gradients of EGL-20 and CWN-1 do not provide positional information to the migrating QR descendants. There is, however, a difference in the ability of EGL-20 and CWN-1 to promote the migration of the QR descendants when these Wnt ligands are overexpressed.

The Wnt Receptors MOM-5/Frizzled and CAM-1/Ror2 Act in Parallel Genetic Pathways to Promote Anterior Migration of the QR Descendants

Analysis of Wnt receptor mutants showed that the QR.pax are posteriorly displaced in mutants of the Frizzled *mom-5* and the Ror2 ortholog *cam-1* (Figure 1B) (Kim and Forrester, 2003; Zinovyeva et al., 2008). *mom-5* has an essential function in early embryogenesis (Thorpe et al., 1997), but homozygous null mutant offspring of heterozygous mothers (*mom-5* [+M]) is viable. Despite this maternal contribution, *mom-5* (+M) mutants exhibit a highly penetrant QR.pax undermigration phenotype. To investigate whether *mom-5* acts cell-autonomously in QR descendant migration, we first examined whether *mom-5* is expressed in the QR lineage. Using a quantitative single-molecule mRNA fluorescent in situ hybridization (smFISH) method (Ji et al., 2013; Middelkoop et al., 2012), we found that *mom-5* is expressed in the Q neuroblasts and their descendants (Figure 1C). Quantification of *mom-5* mRNA spots revealed that *mom-5* is expressed at a significantly higher level in the QR descendants than in the lineally equivalent QL descendants, which is consistent with the observation that *mom-5* mutants are defective in QR but not QL descendant migration (Zinovyeva et al., 2008). Furthermore, we found that the expression of *mom-5* gradually increases in the QR lineage (average of 2.9 ± 2.2 transcripts in QR, 7.8 ± 6.2 transcripts in QR.p, and 21 ± 4.6 transcripts in QR.pa, $n > 20$) (Figure 1D; Figure S1D).

To investigate whether *mom-5* is required in the QR descendants, we used the *egl-17* promoter to specifically express wild-type *mom-5* in the Q lineage of *mom-5* (+M) mutants (Burdine et al., 1998; Ou and Vale, 2009). As shown in Figure 1E, this significantly rescued QR.pax migration. Furthermore, we found that Q lineage-specific knockdown of *mom-5* by *egl-17* promoter directed expression of *mom-5* double-stranded RNA (dsRNA) resulted in a weak but significant undermigration of the QR.pax (Figure 1E). We conclude that *mom-5* functions cell-autonomously in QR descendant migration.

Mutation of the Ror2 ortholog *cam-1* also induced significant undermigration of the QR.pax (Figure 1B) (Kim and Forrester, 2003; Zinovyeva et al., 2008). The penetrance of this phenotype was lower than in *mom-5* (+M) mutants, however, and the QR.pax also localized in a broader region along the anteroposterior axis. To investigate whether the kinase domain of CAM-1 is required for QR descendant migration, we determined QR.pax localization in *cam-1* alleles that mutate (*xd13*) or delete (*ks52*) the kinase domain (Kim and Forrester, 2003). In both *cam-1* alleles, the QR.pax were posteriorly displaced (Figure S1B), but the penetrance of this phenotype was lower than in the *cam-1(gm122)* null mutant, indicating that CAM-1 has both kinase-dependent and kinase-independent functions in QR descendant migration. Examination of endogenous *cam-1* expression showed that *cam-1* is expressed in the Q neuroblast lineage (Figure 1C). Similar to *mom-5*, *cam-1* was expressed at a significantly higher level in the QR descendants than in the QL descendants, which is in agreement with the requirement of *cam-1* for QR but not QL descendant migration (Zinovyeva et al., 2008). Furthermore, we found that the expression of *cam-1* also

gradually increases during QR lineage progression (average of 5.3 ± 3.3 mRNA spots in QR, 5.5 ± 4.8 mRNA spots in QR.p and 17 ± 5.2 mRNA spots in QR.pa, n > 20) (Figure 1D; Figure S1D). To investigate whether *cam-1* is required in the QR descendants, we knocked down *cam-1* by Q lineage specific expression of *cam-1* dsRNA. As shown in Figure 1E, this resulted in weak but significant QR.pax undermigration, consistent with a cell-autonomous function of *cam-1* in QR descendant migration.

To examine whether *mom-5* and *cam-1* are part of a common signaling mechanism or of parallel pathways, we examined *mom-5* (+M); *cam-1* double mutants (Figure 1B). We found that the final position of the QR.pax was shifted toward the posterior, indicating that loss of both receptors enhances the defect in QR descendant migration. In addition, the more widespread distribution of the QR.pax observed in *cam-1* single mutants was retained in the double mutant. We conclude that *mom-5* and *cam-1* act in parallel to control QR descendant migration.

Next, we investigated the genetic relationship between the two receptors and the different Wnt ligands involved in QR descendant migration. We found that the undermigration phenotype of *mom-5* (+M) was strongly enhanced by mutation of *egl-20*, indicating that *mom-5* and *egl-20* act in parallel genetic pathways (Figure 1B). In contrast, there was only weak (but statistically significant) enhancement in double mutants with *cwn-1*. A similar analysis showed that the undermigration phenotype of *cam-1* was strongly enhanced by mutation of *cwn-1*, whereas the *cam-1*; *egl-20* double mutant was not significantly different from *cam-1* single mutants ($p = 0.45$, Fisher's exact test). Mutation of *cwn-2* weakly enhanced the *cam-1* induced undermigration phenotype, but the *cwn-2*; *mom-5* (+M) double mutant was not significantly different from the *mom-5* (+M) single mutant ($p = 0.61$, Fisher's exact test) (Figure S1A). On the basis of these results, we conclude that *egl-20* predominantly acts through the *cam-1* pathway, whereas *cwn-1* (and possibly *cwn-2*) act mainly through the *mom-5* pathway.

The cytoplasmic protein Disheveled (Dvl) is a common component of both canonical and noncanonical Wnt signaling pathways (Angers and Moon, 2009). To investigate whether the parallel *cam-1* and *mom-5* pathways act through distinct Dvl isoforms, we assayed QR descendant migration in null mutants of the three Dvl orthologs *dsh-1*, *dsh-2*, and *mig-5* (Figure S1C). We found that the QR.pax localized at more posterior positions in *dsh-2* (+M) single mutants. Furthermore, double-mutant combinations of the different Wnt and Dvl mutants showed that *dsh-2* and *mig-5* enhance the undermigration phenotype of *egl-20* as well as *cwn-1* and *cwn-2*, indicating that they may act in both of the parallel pathways. This is consistent with the multifunctional nature of Dvl proteins in Wnt signal transduction (Gao and Chen, 2010).

MOM-5/Frizzled and CAM-1/Ror2 Control Distinct Dynamic Aspects of the Long-Range Migration of QR.p

The migration of QR.p and its descendants can be divided into a long-range migration phase in which QR.p and QR.pa cover a total distance of about 38 μm along the anteroposterior body axis (29.2 ± 5.5 μm for QR.p and 8.9 ± 2.5 μm for QR.pa, n > 70) and a short-range migration phase in which QR.paa and QR.pap localize to their final anteroposterior and dorsoventral positions (Figure 1A). We found that the distance of QR.p migration was strongly reduced in *egl-20*, *cwn-1*, *cam-1*, *mom-5* (+M), and *dsh-2* (+M) mutants (Figure S2B), indicating that the CAM-1/Ror2- and MOM-5/Frizzled-dependent Wnt pathways are required for the long-range anterior migration of QR.p.

To examine dynamic aspects of QR.p migration, we performed static and time-lapse spinning-disc confocal imaging on animals in which the plasma membrane and nucleus of the Q neuroblasts and seam cells are marked with GFP (Middelkoop et al., 2012). Expression of these markers (a pleckstrin homology domain containing GFP and a fusion of histone 2B with GFP) do not influence the migration of the QR descendants (Middelkoop et al., 2012). We found that QR.p and its sister cell QR.a polarize along the anteroposterior axis during their migration. At the anterior side, a leading edge is visible at which small filopodia-like protrusions are formed, while the nucleus is positioned in the posterior half of the cell (Figure 2A; Movies S1 and S2). Furthermore, we found that the F-actin-binding protein COR-1/coronin, which marks the leading edge of migrating cells (Wang et al., 2013), is enriched at the anterior side of QR.p and QR.a (Figure S2A). To quantify QR.p polarity, we took the ratio of the distance of the nucleus to the most posterior and the most anterior side of the cell (Figure 2K). In wild-type animals, QR.p was predominantly polarized toward the anterior (ratio of 0.65 ± 0.02, mean ± SEM).

We found that this anterior polarization is lost in *cam-1* mutants (Figure 2D). Time-lapse imaging showed that QR.p and QR.a fail to maintain an anterior protrusion. Instead, the cells flip back and forth between anterior and posterior polarization (Movie S3), a behavior that is captured in the quantification of static images as a large spread in QR.p polarity ratios and a mean polarity ratio (0.92 ± 0.06) that approaches random polarization (Figure 2K). Furthermore, COR-1 was localized to both the anterior and posterior sides of QR.p (Figure S2A). Consistent with our observation that *egl-20* and *cam-1* are part of the same genetic pathway, we found that the polarization and migration of QR.p were similarly affected in *egl-20* mutants (Figures 2B, 2K, and 2M; Movie S4). We conclude that *egl-20* and *cam-1* are required for the persistent anterior polarization of QR.p.

In contrast, measurements of QR.p polarity in *cwn-1*, *cwn-2*, and *mom-5* (+M) mutants showed that the average polarization direction (0.71 ± 0.04, 0.68 ± 0.02, and 0.68 ± 0.03 for *mom-5* [+M], *cwn-1*, and *cwn-2*, respectively) is not significantly different from wild-type (although it should be noted that polarization was more variable in *cwn-2* and *mom-5* mutants; $p < 0.001$, Levene's test) (Figures 2C, 2E, and 2K; Figure S2C) and that COR-1 is normally localized at the anterior side of the cell (Figure S2A). Furthermore, time-lapse imaging revealed that QR.p and QR.a remain correctly polarized toward the anterior in *mom-5* (+M) mutants (Movie S5). The overall speed of migration, however, was significantly reduced (Figure 2L). The absence of a polarity phenotype in *cwn-1*, *cwn-2*, and *mom-5* (+M) mutants is in agreement with the notion that these genes function in a common pathway that is functionally distinct from the *egl-20*- and *cam-1*-dependent pathway. This conclusion is further supported by the observation that loss of *cwn-1* does not significantly change the QR.p polarity phenotype of *egl-20* mutants (Figure S2C).

It has previously been shown that a gain-of-function (gof) mutation of the Rac family member *mig-2* affects the persistent

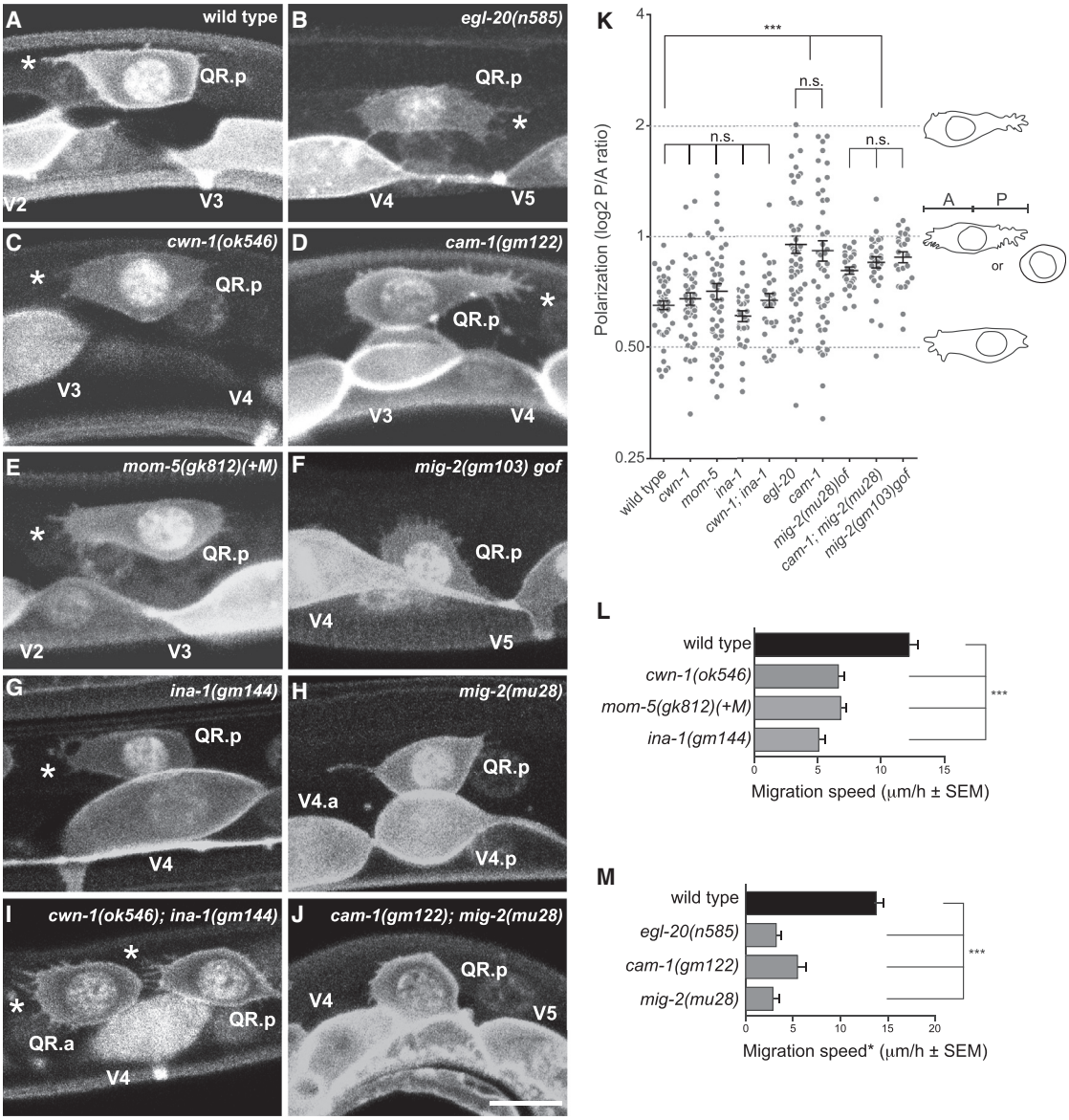

Figure 2. *egl-20*/Wnt and *cam-1*/Ror2 Are Required for Persistent Polarization of QR.p

(A–J) Representative images of migrating QR.p cells in wild-type and mutant animals in which QR.p and the seam cells express plasma membrane and nuclear localized GFP (*hels63*). Anterior is left. Asterisk (white) indicates the main protruding front (if any). Scale bar represents 5 μm.

(K) Quantification of QR.p polarity as the ratio of the distance of the nucleus to the posterior (P) and the anterior (A) side of the cell. Black lines indicate mean ± SEM (n > 25 for all genotypes). Statistical significance was calculated using an unpaired t test (***p < 0.0001). The mean polarity of *cwn-1*, *mom-5*, *ina-1*, and *cwn-1*; *ina-1* double mutants was not statistically different from wild-type.

(L and M) The speed of QR.p migration was calculated from the average anterior distance that QR.p covers in 1 hr (*or 2 hr in M) after the start of migration (n > 75, except *cam-1* n > 50). Statistical significance was calculated using an unpaired t test (***p < 0.0001).

See also Figure S2.

polarization of the QL descendant QL.ap, while mutation of the integrin α-subunit gene *ina-1* affects the speed of QL.ap migration independently of polarity (Ou and Vale, 2009). It was therefore proposed that *mig-2* and *ina-1* function in distinct pathways that separately control the polarity and speed of QL.ap. On the basis of the similarity of the *cam-1* mutant phenotype to *mig-2*(gof) and *mom-5* to *ina-1*, we hypothesized that the *cam-1* pathway may localize the activity of Rac proteins such as MIG-2, while the *mom-5* pathway may regulate migration speed by controlling integrin dynamics. Consistent with the study of Ou and Vale (2009), we found that loss of *ina-1* reduced QR.p migration speed without affecting QR.p polarity (Figures 2G, 2K, and 2L; Movie S6). Because *mom-5*; *ina-1* double mutants were not viable, we examined QR.p polarity in *cwn-1*; *ina-1* double mutants. We found that the double mutant had a similar average QR.p polarity ratio as observed in the *cwn-1* and *ina-1* single

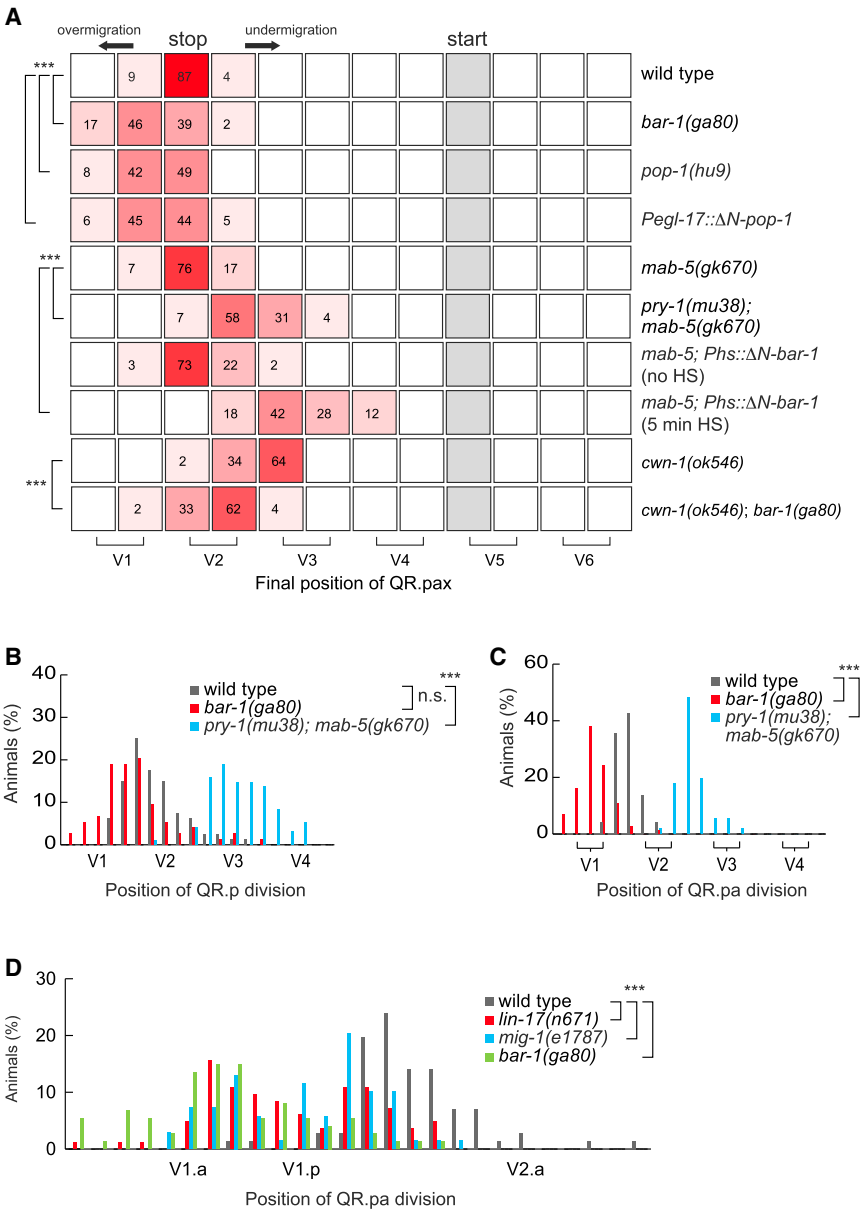

Figure 3. Canonical Wnt/β-catenin Signaling Acts Cell Autonomously to Terminate Migration of QR.pa

(A) Average position of the QR descendants QR.pap and QR.paa with respect to the seam cells V1.a to V6.p (n > 50 for all genotypes).

(B) Position of QR.p division with respect to the seam cells V1 to V4 (n > 75 for all genotypes).

(C) Position of QR.pa division with respect to the seam cells V1 to V4 (n > 70 for all genotypes).

(D) Position of QR.pa division with respect to the seam cells V1.p to V2.a (n > 70 for all genotypes).

In all cases, statistical significance was calculated using Fisher's exact test (***p < 0.0001). See also Figure S3.

mutants (Figures 2I and 2K). The final position of QR.p, however, was shifted posteriorly (Figure S2B), indicating that the defect in QR.p migration is enhanced in the double mutant. The lack of a polarity phenotype in the *cwn-1*; *ina-1* double mutant shows that both genes are dispensable for QR.p polarization. The enhanced defect in QR.p migration suggests, however, that the CWN-1 and MOM-5 dependent Wnt pathway and INA-1 control the migration separately (although it should be noted that a shared function cannot be ruled out because the *ina-1(gm144)* allele is a hypomorphic mutation).

We found that QR.p did not form a clear leading edge and was mostly unpolarized in *mig-2(mu28)* loss-of-function and *mig-2(gm103)* gof mutants (Figures 2F, 2H, and 2K; Movies S7 and S8). Furthermore, QR.p was mostly unpolarized in the *cam-1*; *mig-2(mu28)* double mutant, a phenotype that was quantitatively similar to the *mig-2(mu28)* single mutant (Figures 2J and 2K). The suppression of the random polarization phenotype of *cam-1* indicates that *mig-2* functions downstream of *cam-1*. This suppression could be related to a general requirement of MIG-2 for protrusion formation, but is also in agreement with our model that the CAM-1 pathway may control the persistent polarization of QR.p by regulating the activity of MIG-2. However, we found that the QR.p migration defect of the *cam-1*; *mig-2(mu28)* double mutants was enhanced compared with the single mutants (Figure S2B), indicating that in addition to this potentially shared function in QR.p polarization, CAM-1 and MIG-2 also have separate functions in QR.p migration.

Taken together, these results support our conclusion that the Wnt receptors CAM-1/Ror2 and MOM-5/Frizzled function in parallel to control the long-range anterior migration of QR.p. Furthermore, our results demonstrate that CAM-1 and MOM-5 mediate distinct dynamic aspects of the migration, with the CAM-1 pathway regulating the persistent polarization of QR.p and the MOM-5 pathway controlling migration independently of polarity.

Termination of QR.pa Migration Requires Activation of Canonical Wnt/β-catenin Signaling

The long-range anterior migration of the QR descendants ends when QR.pa divides at a position between the seam cells V1.p and V2.a (Figure 1A). To investigate how QR.pa is instructed to stop at this specific position, we examined mutants in which the QR descendants migrate beyond their wild-type positions. Again using the final position of QR.paa and QR.pap as a proxy for total migration distance, we found that the QR.pax overmigrate in mutants of the canonical β-catenin gene *bar-1* (Figure 3A), as has been observed previously (Whangbo and Kenyon, 1999). β-catenin is a central component of the canonical Wnt/β-catenin pathway that binds to members of the TCF

family of transcription factors to coactivate the expression of Wnt target genes (Clevers and Nusse, 2012). We found that mutation of the single *C. elegans* TCF ortholog *pop-1* induces a similar overmigration phenotype as *bar-1*. Furthermore, specific expression of dominant-negative N-terminally truncated POP-1 (Korswagen et al., 2000) in the Q cell lineage induced significant overmigration as well (Figure 3A), demonstrating that *pop-1* functions cell-autonomously in QR descendant migration.

The overmigration observed in *bar-1* and *pop-1* mutants indicates that activation of canonical Wnt/β-catenin signaling may be required to stop migration of the QR descendants. To test this possibility, we expressed constitutively active N-terminally truncated BAR-1 using a HS inducible promoter (Gleason et al., 2002) and asked whether early activation of Wnt/β-catenin signaling prematurely terminates QR descendant migration. To prevent activation of the posterior migration pathway that is induced by Wnt/β-catenin signaling in the QL lineage, we performed these experiments in animals carrying a null mutation in the Wnt target gene *mab-5* (Figure 3A) (Korswagen et al., 2000; Maloof et al., 1999; Salser and Kenyon, 1992). Consistent with our hypothesis, we found that a brief HS at the beginning of the migration process leads to significant undermigration of the QR.pax (Figure 3A). A similar result was obtained when we constitutively activated Wnt/β-catenin signaling by introducing a mutation in the negative regulator *pry-1*/Axin (Korswagen et al., 2002).

To directly examine the effect of canonical Wnt/β-catenin signaling on the long-range migration of QR.p and QR.pa, we determined the position at which these cells end their migration in wild-type and Wnt/β-catenin pathway mutants. In *bar-1* mutants, the position at which QR.p terminates its migration and divides was not significantly different from wild-type (Figure 3B) ($p = 0.1$, Fisher's exact test). In contrast, there was significant overmigration of QR.pa, with the majority of cells dividing at a more anterior position than in wild-type animals (Figures 3C and 3D). The opposite phenotype was observed when Wnt/β-catenin signaling was constitutively activated by mutation of *pry-1*, with both QR.p and QR.pa terminating their migration at a more posterior position than in wild-type animals (Figures 3B and 3C). The short-range anteroposterior migration of QR.paa and QR.pap was not affected in *bar-1* mutants (Figure S3). We conclude that canonical Wnt/β-catenin signaling is necessary and sufficient to inhibit the long-range anterior migration of the QR descendants.

The specific effect of *bar-1* on QR.pa migration indicates that canonical Wnt/β-catenin signaling is activated at the end of the long-range migration phase to terminate QR.pa migration. To further investigate this model, we determined QR.p migration speed and the final localization of the QR.pax in double mutants between *bar-1* and the QR.p migration mutant *cwn-1*. We found that the speed of QR.p migration was similar as in the *cwn-1* single mutant (Figure 5C). The final position of the QR.pax was however intermediate to the overmigration induced by *bar-1* and the undermigration induced by *cwn-1* (Figure 3A). We conclude that long-range anterior migration (noncanonical Wnt signaling) and termination of anterior migration (canonical Wnt/β-catenin signaling) are separate and sequentially acting processes.

MIG-1/Frizzled Is Necessary and Sufficient for Termination of QR.pa Migration and Is Strongly Upregulated at the End of the Long-Range Migration Phase

To investigate how QR.pa migration is regulated at the Wnt receptor level, we determined the position at which QR.pa divides in Frizzled mutants. We found that there was extensive overmigration of QR.pa in *mig-1* and *lin-17* mutants (Figure 3D). As in *bar-1* mutants, QR.p migration was not significantly affected (Figure S2B), indicating that *mig-1* and *lin-17* are specifically required for the canonical Wnt/β-catenin pathway-dependent termination of QR.pa migration. This is in agreement with the role of MIG-1 and LIN-17 in activation of canonical Wnt/β-catenin signaling in the QL neuroblast lineage (Harris et al., 1996; Ji et al., 2013; Maloof et al., 1999).

Consistent with a cell-autonomous function of *mig-1* and *lin-17* in migration termination, we found that both receptors are expressed in the QR.pa neuroblast (Figure 4A). However, quantification of *mig-1* and *lin-17* smFISH spots revealed that there are important differences in the temporal expression of the two receptors during QR lineage progression. We found that the expression of *lin-17* is relatively constant (average of 9.3 ± 4.7 transcripts in QR, 4.5 ± 1.6 transcripts in QR.p and 4.0 ± 1.6 transcripts in QR.pa, $n > 20$) (Figure 4B; Figure S1D). The expression of *mig-1*, on the other hand, is highly dynamic, with an initial expression of 19 ± 8.1 transcripts in QR, an almost complete loss of expression (1.2 ± 0.4) in QR.p and a striking 18-fold upregulation of expression (21 ± 1.2) in QR.pa ($n > 25$) (Figure 4B; Figure S1D).

The upregulation of *mig-1* at the end of the long-range anterior migration phase suggests that *mig-1* may act as a switch that turns on Wnt/β-catenin signaling to stop anterior migration. To test this model, we asked which of the two phases of *mig-1* expression is required for the correct positioning of the QR.pax. We found that expression of *mig-1* using the *egl-17* promoter, which recapitulates the early expression of *mig-1* in QR (Figure 4C; Figure S1D), did not rescue the overmigration phenotype of *mig-1* mutants (Figure 4D). In contrast, the overmigration phenotype was fully rescued when *mig-1* was specifically expressed in QR.pa using the *egl-46* promoter (Wu et al., 2001). Next, we examined whether expression of *mig-1* is sufficient to stop anterior migration. To test this, we used the *mom-5* promoter to express *mig-1* during QR.p migration. Consistent with our model, we found that such premature expression of *mig-1* resulted in significant undermigration of the QR.pax. We conclude that the upregulation of *mig-1* expression is necessary and sufficient to stop the anterior migration of QR.pa.

mig-1 Expression Is Activated through a Q Lineage-Intrinsic Timing Mechanism

Next, we investigated how the expression of *mig-1* is induced in QR.pa. One possibility is that positional cues, provided by localized or graded signals, induce *mig-1* expression at a specific position along the anteroposterior axis. An alternative possibility is that *mig-1* expression is regulated through a Q lineage-intrinsic mechanism that turns on *mig-1* expression at a specific time in the migration process. To distinguish between these two possibilities, we first asked whether posterior displacement of QR.p and QR.pa interferes with *mig-1* expression. In gof mutants of

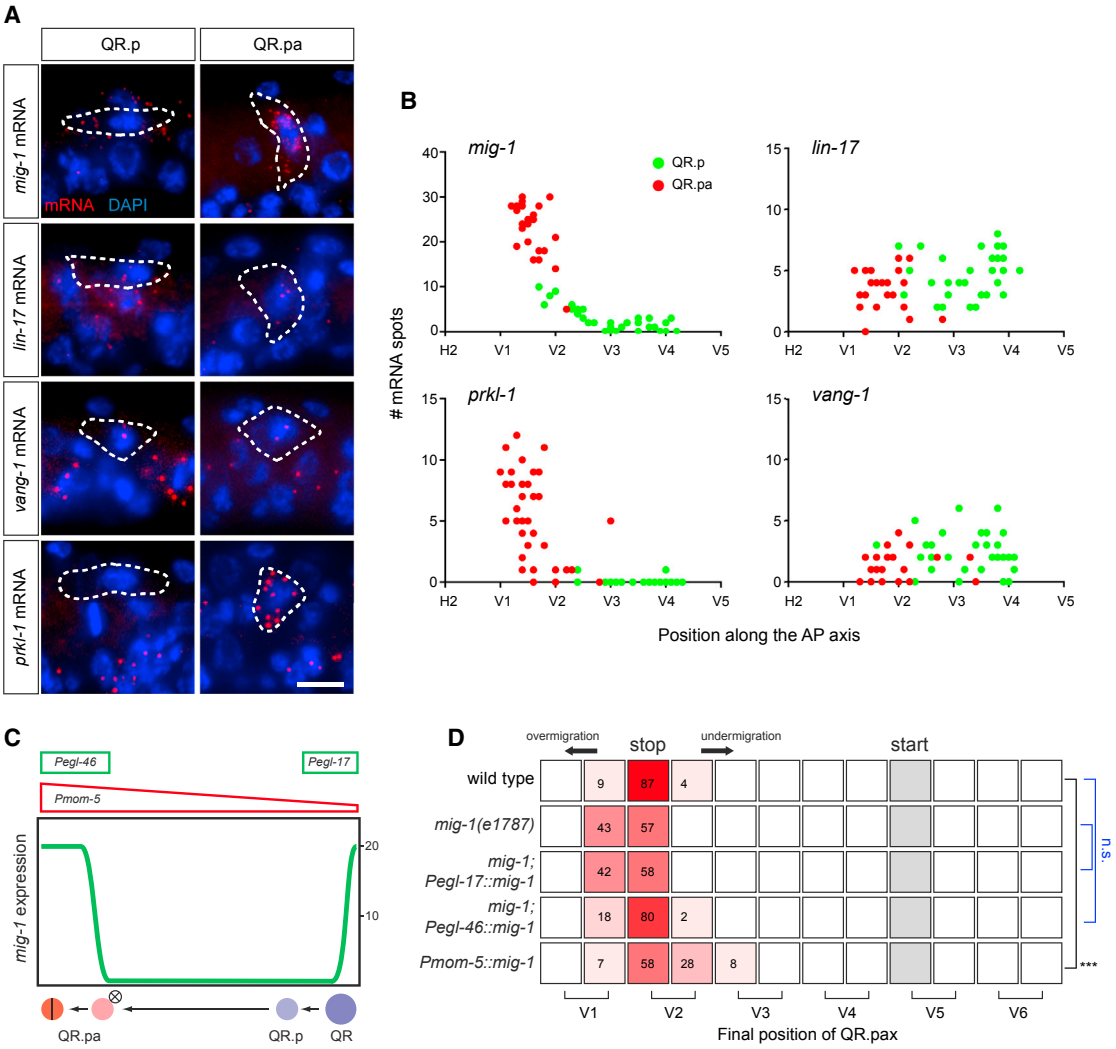

Figure 4. Upregulation of *mig-1*/Frizzled Expression in QR.pa Is Necessary and Sufficient to Terminate QR.pa Migration

(A) smFISH analysis of endogenous *mig-1*, *lin-17*, *vang-1*, and *prkl-1* mRNA in QR.p and QR.pa. Images of QR.p and QR.pa were taken in synchronized populations grown for 5 to 6 and 7 to 8 hr after hatching, respectively. Nuclei are visualized with DAPI staining. Scale bar represents 5 μm.

(B) *mig-1*, *lin-17*, *vang-1*, and *prkl-1* transcription dynamics in single QR.p (green) and QR.pa (red) neuroblast daughter cells as measured in wild-type animals (n > 55 for each mRNA species). The number of mRNA spots per cell is plotted against the cell position with respect to the seam cells H2 to V5.

(C) Schematic overview of *mig-1* transcription dynamics in QR and its descendants during their migration in wild-type animals. Expression is initially high in QR and then drops quickly during initial migration. In QR.p expression is low and rises sharply again in QR.pa. On top of the graph, the transcription dynamics of *egl-17*, *egl-46*, and *mom-5* are indicated.

(D) Average position of the QR descendants QR.pap and QR.paa with respect to the seam cells V1.a to V6.p (n > 50 for all genotypes). Statistical significance was calculated using Fisher's exact test (***p < 0.0001).

mig-2, the anterior migration of QR.p is reduced (Ou and Vale, 2009), and the final position of QR.p and QR.pa is shifted about two seam cell positions to the posterior. We found that despite this difference in position along the anteroposterior axis, *mig-1* expression is still activated at wild-type levels in QR.pa (Figure 5A). Next, we investigated whether anterior displacement of the QR descendants influences *mig-1* expression. QR.p and QR.pa migrate beyond their normal positions when EGL-20 is overexpressed using a heat-inducible promoter (Figures 5A and 5B) (Whangbo and Kenyon, 1999). We found that when QR.p and QR.pa are shifted toward the anterior, *mig-1* is also expressed more anteriorly (Figure 5A). Taken together, these results demonstrate that the upregulation of *mig-1* expression in QR.pa is not induced by positional cues.

The second possibility is that *mig-1* expression is regulated through a Q lineage-intrinsic mechanism. We hypothesized that *mig-1* expression is induced by a timing mechanism that either counts total migration time or is coupled to the cell cycle of QR.p and QR.pa. In such a model, the position at which *mig-1* expression is induced and QR.pa migration is terminated will depend on the overall speed of migration: when migration speed is reduced, *mig-1* will be expressed more posteriorly, and when speed is increased, *mig-1* will be expressed more anteriorly. This model is supported by the observation that in

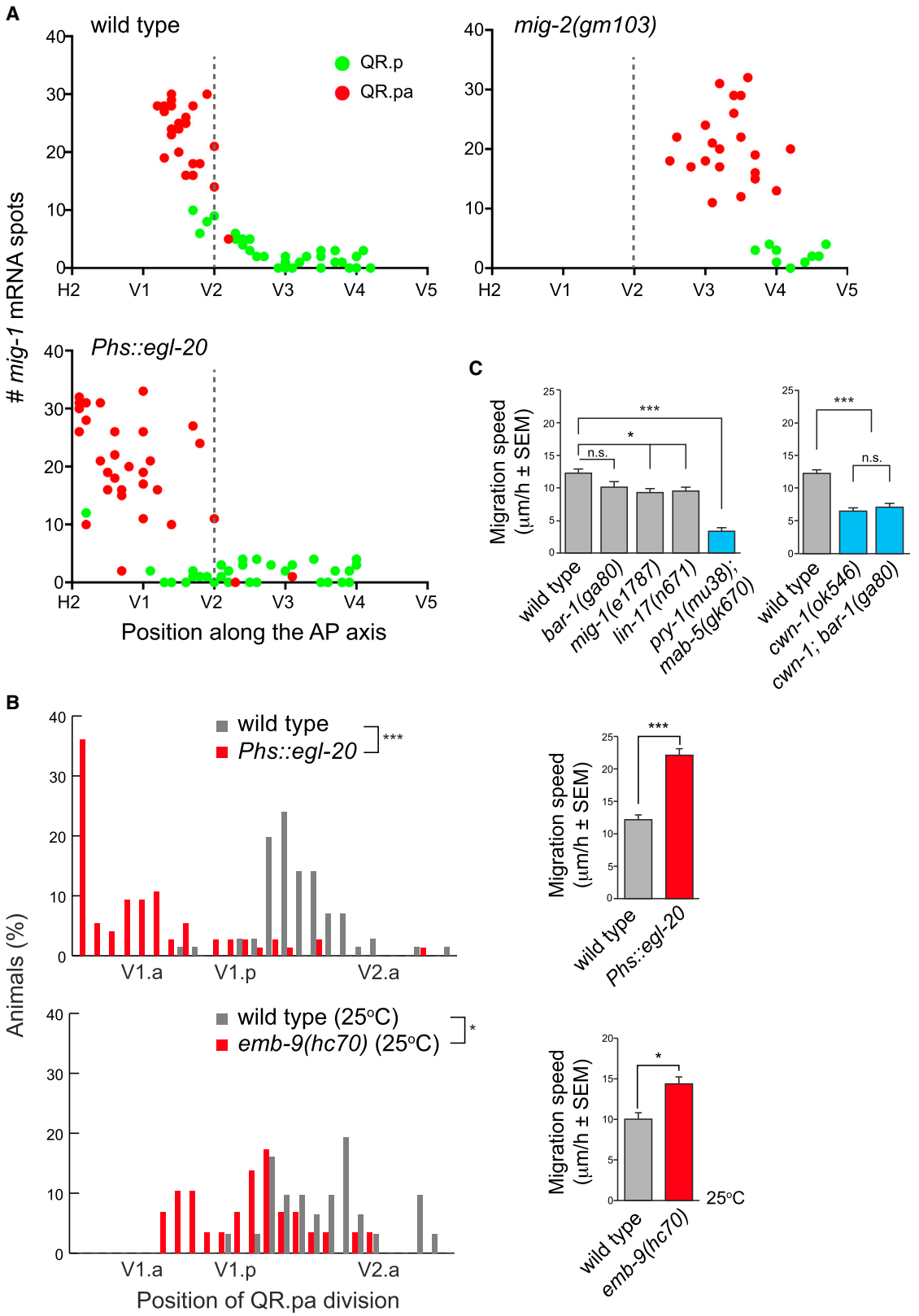

(legend on next page)

mig-2(gof) mutants, which express *mig-1* at a more posterior position than in wild-type (Figure 5A), the speed of migration is strongly reduced (Ou and Vale, 2009). Furthermore, we found that overexpression of EGL-20, which leads to overmigration of QR.pa and more anterior *mig-1* expression, induces a significant increase in migration speed (Figure 5B). A similar correlation between migration speed and QR.pa overmigration was observed in the collagen mutant *emb-9* (Figure 5B), which may facilitate migration by providing a less dense extracellular matrix (C. Kenyon, personal communication).

The speed of QR.p migration was not increased in *mig-1*, *lin-17*, and *bar-1* mutants (Figure 5C), which is consistent with our model that canonical Wnt/β-catenin signaling is required for termination of QR.pa migration and not for the anterior migration process itself. On the basis of these results, we conclude that the endpoint of QR.pa migration is defined by the combined regulation of migration speed and the timing of *mig-1* expression and canonical Wnt/β-catenin pathway activation.

The Final Short-Range Migration of QR.pap and QR.paa Is Dependent on the PCP Components VANG-1/Vangl and PRKL-1/Pk

The last phase of QR descendant migration involves the short-range migration of the QR.pa daughter cells QR.pap and QR.paa (Figure 1A). Measurements of the final position of QR.pap and QR.paa showed that QR.pap localizes slightly anterior to the position of QR.pa division, while QR.paa migrates a short distance toward the posterior (Figures 6A and 6A′). In addition, QR.pap moves to a specific dorsal position, where it differentiates into the neuron SDQR, while QR.paa migrates ventrally and differentiates into the neuron AVM (Figure 6C) (Hedgecock et al., 1987; Sulston and Horvitz, 1977).

In a small-scale screen of noncanonical Wnt pathway components (data not shown), we found that the average position of QR.paa and QR.pap was shifted toward the anterior in mutants of the PCP pathway components *vang-1*/Vangl and *prkl-1*/Pk (Figure S4A). Both genes likely function in the same pathway, as the QR.pax were similarly localized in *vang-1*; *prkl-1* double mutants. Detailed analysis of the final localization of the individual QR descendants in *vang-1* and *prkl-1* mutants showed that the position of QR.pa division was not significantly different from wild-type ($p = 0.97$ and 0.10, Fisher's exact test, respectively) (Figure 6B), indicating that *vang-1* and *prkl-1* do not affect the canonical Wnt/β-catenin pathway dependent termination of QR.pa migration. Instead, we found that *vang-1* and *prkl-1* are required for the final positioning of QR.paa and (to a lesser extent) of QR.pap (Figure 6B). Thus, in *vang-1* and *prkl-1* mutants, the short-range posterior migration of QR.paa was absent, with QR.paa either remaining at its starting position or moving slightly anterior (Figure 6A″). In the case of QR.pap, there was a slight but significant anterior shift in the final position.

We found that *vang-1* and *prkl-1* are also required for the dorsoventral positioning of QR.pap and QR.paa, with both cells showing either reduced or even reversed migration along the dorsoventral axis (Figure 6C). It has previously been shown that the dorsoventral position of QR.pap is regulated by UNC-6/netrin and the receptors UNC-5 and UNC-40/DCC (Kim et al., 1999). We confirmed the requirement of *unc-6* for the dorsal migration of QR.pap but found that the ventral migration of QR.paa was also significantly affected in *unc-6(e78)* hypomorphic and *unc-6(ev400)* null mutants (Figure 6C; Figure S4C). In double mutants between *unc-6(ev400* or *e78)* and *prkl-1*, the dorsoventral distribution of QR.pap and QR.paa was not significantly different from *unc-6* single mutants ($p = 0.58$ and 0.13, unpaired, two-tailed t test, respectively, for *ev400*). Comparable results were obtained with *unc-6*; *vang-1* double mutants. The absence of an enhanced dorsoventral migration phenotype in double mutants of *prkl-1* and *vang-1* with *unc-6* suggests that these genes may be part of a common genetic pathway. This conclusion is supported by our observation that the expression of the UNC-6 receptor *unc-40* is not influenced by loss of *prkl-1* (Figure S4D).

To determine in which cells *vang-1* and *prkl-1* are expressed during Q neuroblast migration, we performed smFISH analysis in L1 larvae (Figures S4B and S4E). We found that *vang-1* is expressed in both the QL and QR neuroblast lineages. In addition, *vang-1* mRNA was detected in hypodermal seam cells, the M mesoblast cell, and in ventral nerve cord neurons. To investigate whether *vang-1* is required in the migrating QR descendants, we tested whether Q cell lineage-specific expression of *vang-1* rescues QR.paa and QR.pap migration in a *vang-1* null mutant background. Consistent with a cell-autonomous function of *vang-1*, we found that expression of *vang-1* in the Q cell lineage was sufficient to rescue QR.pax migration ($p < 0.0001$, Fisher's exact test) (Figure S4A).

prkl-1 expression was observed in the Q neuroblast descendants, the M mesoblast cell, and at low levels in ventral nerve cord neurons and unidentified cells in the head region (Figure S4B). Consistent with the more prominent role of *prkl-1* in QR.paa migration, we found that *prkl-1* is expressed at a significantly higher level in QR.paa than QR.pap (Figure 6D; Figure S4E). Interestingly, smFISH analysis revealed that the expression of *prkl-1* is dynamically regulated during QR descendant migration. Thus, whereas *vang-1* transcription remained relatively constant throughout QR lineage progression, the expression of *prkl-1* was strongly upregulated at the end of the long-range migration phase (Figure 4B). These results indicate that, similar to the role of *mig-1* in QR.pa migration termination,

Figure 5. A QR Lineage-Intrinsic Mechanism Controls the Termination of QR.pa Migration

(A) *mig-1* transcription dynamics in single QR.p (green) and QR.pa (red) neuroblast daughter cells as measured in wild-type, *mig-2*(gof) mutants and *Phs::egl-20* transgenic animals (heat-shocked for 1 min) ($n > 30$ for all genotypes). The number of mRNA spots per cell is plotted against the cell position with respect to the seam cells H2 to V5. Dashed line indicates the position of seam cell V2.

(B) Left: Position of QR.pa division with respect to the seam cells V1.p to V2.a ($n > 30$ for all genotypes). Statistical significance was calculated using Fisher's exact test (*$p < 0.01$, ***$p < 0.0001$). Right: The speed of QR.p migration was calculated from the average distance that QR.p covers in 1 hr after the start of migration ($n > 75$ for all genotypes). Statistical significance was calculated using an unpaired t test (*$p < 0.01$, ***$p < 0.0001$). EGL-20 expression was induced using a 1 min HS. *emb-9* mutants were shifted to the nonpermissive temperature of 25°C 9 to 10 hr prior to analysis.

(C) Speed of QR.p migration in wild-type and mutant animals ($n > 75$, except *pry-1*; *mab*-5, $n > 50$) (*$p < 0.01$, ***$p < 0.0001$).

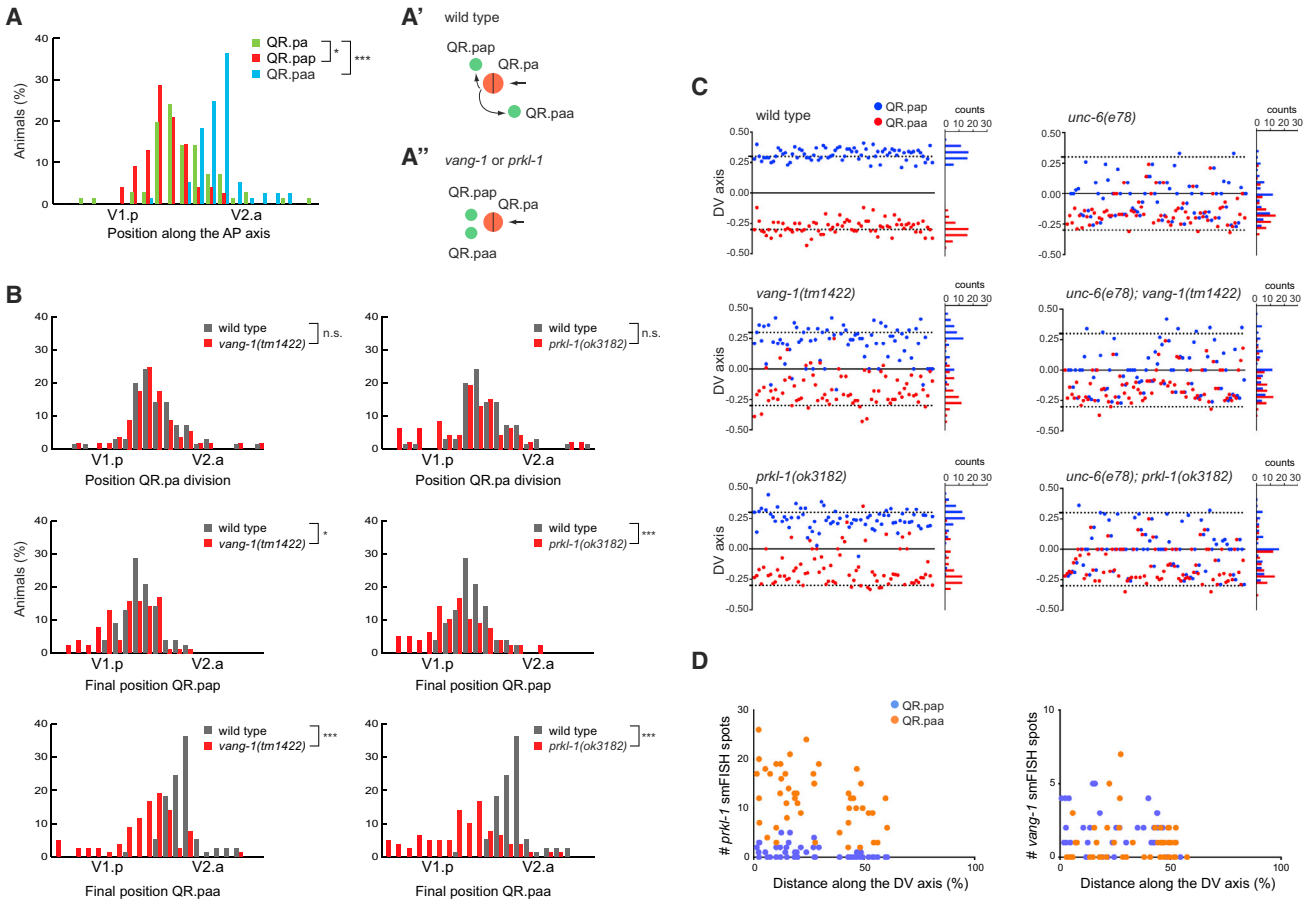

Figure 6. The PCP Pathway Components *vang-1*/Vangl and *prkl-1*/Pk Control the Final Short-Range Migration of QR.pap and QR.paa

(A) Position of QR.pa, QR.pap, and QR.paa relative to the seam cells V1.p to V2.a in wild-type animals (n > 70 for all cell types). Statistical significance was calculated using Fisher's exact test (*p < 0.01, ***p < 0.0001).

(A′ and A′′) Schematic representation of the short-range anteroposterior and dorsoventral migration of QR.paa and QR.pap in wild-type and *vang-1* and *prkl-1* mutants.

(B) Position of QR.pa, QR.pap, and QR.paa relative to the seam cells V1.p to V2.a in wild-type and mutant animals (n > 70 for all genotypes; *p < 0.01, ***p < 0.0001).

(C) Position of QR.pap and QR.paa on the dorsoventral axis (n > 70 for all genotypes). Midline is set at zero, and dashed lines indicate the average position of QR.pap and QR.paa in wild-type. The histogram on the right displays percentile counts along the dorsoventral axis.

(D) *prkl-1* and *vang-1* transcription dynamics in single QR.pap (blue) and QR.paa (yellow) neuroblast daughter cells as measured in wild-type animals (n > 45 for both cell types). The number of mRNA spots per cell is plotted against the relative distance between the two QR.pax cells with respect to the total width of the dorsoventral axis, with a longer distance correlating to more advanced stages of dorsoventral migration.

See also Figure S4.

upregulation of *prkl-1* expression may mediate the transition to the final short-range migration phase. In support of this model, we found that early expression of *prkl-1* in the QR lineage using the *egl-17* promoter did not rescue QR.pap and QR.paa migration in *prkl-1* null mutants (p = 0.11, Fisher's exact test), while expression using the *egl-46* promoter, which is expressed late in the QR lineage, fully rescued the migration phenotype (p < 0.0001, Fisher's exact test) (Figure S4A).

DISCUSSION

Wnt proteins play an evolutionarily conserved role in guiding migrating cells and axons along the anteroposterior axis of the developing nervous system. In *C. elegans*, the anterior migration of the QR neuroblast descendants requires the activity of multiple Wnt ligands and receptors (Harterink et al., 2011; Kim and Forrester, 2003; Zinovyeva and Forrester, 2005; Zinovyeva et al., 2008). Here, we have investigated how the QR descendants integrate this complex information to migrate to their precisely defined final positions. We found that the migration is divided into three sequential steps, each of which is mediated by a distinct Wnt signaling mechanism. Importantly, our results show that the QR descendants switch between these signaling mechanisms by temporally regulating the expression of Wnt pathway components.

Wnt proteins form concentration gradients that can act as attractive or repulsive guidance signals for migrating cells and axons in the developing nervous system (Zou and Lyuksyutova,

2007). The Wnt ligands that are required for QR descendant migration, EGL-20 and CWN-1, are expressed in the posterior body region and are expected to form posterior-to-anterior concentration gradients, as has been shown for EGL-20 (Coudreuse et al., 2006; Harterink et al., 2011; Pan et al., 2006; Whangbo and Kenyon, 1999). However, we found that neither of the two Wnt ligands provides positional information to the migrating QR descendants, as uniform expression or even reversal of the EGL-20 and CWN-1 concentration gradients is sufficient to restore normal QR.pax positioning in their respective mutant backgrounds. Furthermore, we found that the overmigration of the QR descendants that is induced by overexpression of EGL-20 is a consequence of the dose-dependent effect of EGL-20 on the speed of QR.p migration. The permissive role of EGL-20 and CWN-1 raises the question how the QR descendants are instructed to migrate toward the anterior. Previous studies have shown that anterior migration of the QR descendants requires the transmembrane protein MIG-13 (Masuda et al., 2012; Sym et al., 1999). Recent evidence suggests that MIG-13 functions cell-autonomously in the QR descendants to promote anterior migration (Wang et al., 2013). On the basis of these observations and the results presented in this study, we propose that the QR descendants use MIG-13 to respond to an as yet unknown anterior guidance signal, but require Wnt signaling for (1) persistent polarization and motility, (2) termination of anterior migration, and (3) switching to the final dorsoventral migration phase.

The first phase in the migration process is the MOM-5/Frizzled- and CAM-1/Ror2-dependent long-range anterior migration of QR.p and QR.pa. Analysis of mutant combinations showed that CAM-1 and MOM-5 act in parallel pathways that control distinct aspects of the migration process. Using live-cell time-lapse confocal imaging, we found that QR.p fails to persistently polarize in *cam-1* mutants, whereas in *mom-5* mutants, QR.p remains correctly polarized but migrates at a strongly reduced speed. Interestingly, the phenotype of *cam-1* is remarkably similar to the defect in QL.ap polarity observed in gof mutants of the Rac-like small guanosine triphosphatase (GTPase) *mig-2*, while *mom-5* resembles mutants of the integrin alpha-subunit *ina-1* (Ou and Vale, 2009). Analysis of double mutants revealed that the *mom-5* pathway and *ina-1* may function in parallel to control QR.p migration speed. The ectopic protrusion phenotype of *cam-1*, however, was suppressed by loss of *mig-2*, indicating that CAM-1 may control QR.p polarity by regulating the activity of MIG-2. In vertebrates, Ror2 has been shown to regulate filopodia formation (Schambony and Wedlich, 2007) and to control the polarity of migrating cells through reorientation of the microtubule organizing center (Nishita et al., 2010; Nomachi et al., 2008), but a direct link with Rac family GTPases has not been made. The CAM-1 dependent polarization of QR.a and QR.p therefore provides a valuable single cell assay to investigate how Ror2 signaling controls cell polarity and filopodia formation.

The second step in QR descendant migration is termination of the MOM-5 and CAM-1 dependent long-range anterior migration phase. We found that this requires activation of canonical Wnt/β-catenin signaling in QR.pa. Canonical Wnt/β-catenin signaling may terminate migration by directly inhibiting the CAM-1- and MOM-5-dependent migration pathways but may also stop migration by promoting division of QR.pa. Measurements of migration speed in *pry-1*/Axin mutants showed that constitutive activation of Wnt/β-catenin signaling induces a significant reduction in QR.p migration speed (Figure 5C). This is in agreement with a direct role of Wnt/β-catenin signaling in migration inhibition. Interestingly, QR.p was normally polarized in *pry-1* mutants (Figure S2C), indicating that canonical Wnt/β-catenin signaling reduces migration speed independently of QR.p polarization.

The Frizzled *mig-1* plays a pivotal role in defining the endpoint of QR.pa migration. Quantification of *mig-1* expression showed that it is sharply upregulated in QR.pa, and transgenic rescue experiments revealed that this induction of *mig-1* expression is necessary and sufficient for termination of migration. Importantly, we found that the expression of *mig-1* is not induced by positional cues from the extracellular environment. Instead, we found that *mig-1* expression is activated through a cell-intrinsic timing mechanism. Consistent with this mechanism, we found that the position along the anteroposterior axis at which QR.pa expresses *mig-1* is correlated with the speed of migration. An interesting question is how *mig-1* expression is activated at such a specific time point in the migration process. One possibility is that the temporal regulation of *mig-1* expression is coupled to the QR.p lineage, with division of QR.p triggering the expression of *mig-1* in QR.pa, but a lineage-independent time-keeping mechanism may be involved as well.

The final phase in the migration process is the short-range migration of QR.paa and QR.pap. We found that this anteroposterior and dorsoventral migration is dependent on the PCP pathway components VANG-1/Vangl and PRKL-1/Pk. Similar to *mig-1*, the expression of *prkl-1* is temporally regulated, indicating that the transition to this PCP related pathway may also be mediated through a cell-intrinsic timing mechanism. Analysis of dorsoventral migration in double mutant combinations of *vang-1* and *prkl-1* with *unc-6*/Netrin showed that *vang-1* and *prkl-1* may function in a common genetic pathway with the *unc-6* guidance signal. How PCP and UNC-6 Netrin signaling are coordinated to control the final dorsoventral positioning of QR.paa and QR.pap remains to be established.

Transcriptional regulation of guidance receptors and intracellular signaling components is an important mechanism in specifying the complex trajectories of migrating cells and axons (Derijck et al., 2010; Polleux et al., 2007; Su et al., 2000). The expression of such guidance components can be induced by extracellular signals, but our results show that cells can also use cell-intrinsic mechanisms to express distinct Wnt pathway components at specific time points in the migration process. Such cell-intrinsic regulation of migration also appears to be important in vertebrate nervous system development. During brain development, retinal ganglion cell (RGC) axons migrate toward the optic tectum. At a specific stage in their migration, the RGC axons induce the expression of neuropilin-1, which enables them to respond to semaphorin guidance cues (Derijck et al., 2010). The time-dependent induction of neuropilin-1 expression also occurs when RGCs are grown in vitro, indicating that the temporal regulation of neuropilin-1 expression is a cell-autonomous process (Campbell et al., 2001). How neuropilin-1 is upregulated at such a specific time point in RGC development is still unknown. Our observation that QR descendant migration is controlled through temporal regulation of Wnt responsiveness provides a powerful paradigm to study cell-intrinsic timing

mechanisms in a highly reproducible single cell migration system.

EXPERIMENTAL PROCEDURES

Analysis of QR Descendant Migration

The final position of the QR descendants QR.paa and QR.pap was determined using differential interference contrast (DIC) microscopy in late L1 larvae, as described (Coudreuse et al., 2006). The position of QR.paa and QR.pap was determined with respect to the seam cell daughters V1.a to V6.p. To provide a more detailed measure of QR.paa and QR.pap migration distance, the position was determined with respect to the V1.p and V2.a seam cell nuclei. The relative position of QR.paa and QR.pap on the dorsoventral axis was determined by dividing the distance between QR.paa or QR.pap and the midline (defined as the middle of the V1.p nucleus) over the total dorsoventral distance at this position. The position of QR.pa was determined in transgenic animals expressing GFP in the Q cell lineage (transgenes *ayIs9* and *syIs90*). The relative position of QR.pa with respect to the V1.p and V2.a seam cell nuclei was determined by dividing the distance between V1.p and QR.pa over the total distance between V1.p and V2.a. The position of QR.p division was determined relative to the seam cells V1 to V4. The speed of QR.p migration was measured in synchronized larvae by determining the average distance of migration during the first hour after QR division. A 2 hr time frame was chosen for *egl-20*, *cam-1*, and *mig-2(mu28)* mutants to reliably score anterior migration distance.

Imaging

For static imaging, animals were mounted on 2% agarose pads containing 10 mM sodium azide. Confocal images were obtained using a Leica TCS SPE confocal microscope. For imaging of QR.p polarity using the *hels63* marker, settings were 63× objective, 3× zoom, and 15% 488 nm (GFP) laser power. For imaging of the plasma membrane and actin localization in QR.p using the *casIs49* marker, settings were 63× objective, 3× zoom, 20% 488 nm (GFP) laser power, and 20% 532 nm (mCherry) laser power. Z-stacks were made using a 0.5 μm step size. Image acquisition was performed using LASAF software. A maximum projection was made of all slices in which the Q cell was detected. DIC and epifluorescence images were obtained using a Zeiss Axioscope microscope equipped with a Zeiss Axiocam digital camera. Images were analyzed using ImageJ version 1.43u software. For time-lapse imaging, larvae synchronized at 5 to 6 hr after hatching were mounted in 0.5 μl of 0.1 μm diameter polystyrene microspheres in aqueous suspension (Polysciences 00876 2.5% w/v aqueous suspension) onto a 10% agarose pad (Kim et al., 2013). Animals were imaged using a PerkinElmer Ultraview Vox spinning disk confocal microscope (63× objective, 1× zoom, and 4% 488 nm laser power). Z-stacks (0.5 μm) were made every 2 min for a 2 hr duration. Image acquisition was performed using Velocity software. Images were processed and movies were created using Velocity and ImageJ software, respectively.

HS Experiments

HS experiments were performed as previously described (Middelkoop et al., 2012) with the following changes: L1 larvae synchronized at 0 to 1 hr after hatching were incubated at 33°C in a volume of 50 μl for the indicated length of time.

Statistical Analysis

Statistical analysis of QR descendant position was performed using Fisher's exact test. A Monte Carlo approximation, iterated 10,000 times using SPSS version 20, was used to estimate significance. Analysis of differences in QR.p polarity variability was performed using Levene's test for equal variance. In all other cases, statistical analysis was examined using unpaired, two-tailed Student's t tests. Results were deemed significant at $p < 0.05$.

SUPPLEMENTAL INFORMATION

Supplemental Information includes Supplemental Experimental Procedures, four figures, and eight movies and can be found with this article online at http://dx.doi.org/10.1016/j.devcel.2014.08.008.

ACKNOWLEDGMENTS

We thank Erik Jorgensen, Jeroen Pasterkamp, and Martin Harterink for critically reading the manuscript; Sander van den Heuvel, Wayne Forrester, Hitoshi Sawa, Guangshuo Ou, and the Caenorhabditis Genetics Center (University of Minnesota, Minneapolis) for strains; and the Hubrecht Imaging Center for assistance with microscopy. This work was funded by a grant from the Dutch Cancer Society (HUBR 2008-4114) (H.C.K.) and the NIH/National Cancer Institute Physical Sciences Oncology Center at Massachusetts Institute of Technology (U54CA143874), an NIH Pioneer award (DP1CA174420), and an ERC Advanced grant (2011-294325_GeneNoiseControl) (A.v.O.).

Received: March 13, 2014
Revised: July 11, 2014
Accepted: August 7, 2014
Published: October 16, 2014

REFERENCES

Angers, S., and Moon, R.T. (2009). Proximal events in Wnt signal transduction. Nat. Rev. Mol. Cell Biol. *10*, 468–477.

Burdine, R.D., Branda, C.S., and Stern, M.J. (1998). EGL-17(FGF) expression coordinates the attraction of the migrating sex myoblasts with vulval induction in *C. elegans*. Development *125*, 1083–1093.

Campbell, D.S., Regan, A.G., Lopez, J.S., Tannahill, D., Harris, W.A., and Holt, C.E. (2001). Semaphorin 3A elicits stage-dependent collapse, turning, and branching in *Xenopus* retinal growth cones. J. Neurosci. *21*, 8538–8547.

Clevers, H., and Nusse, R. (2012). Wnt/β-catenin signaling and disease. Cell *149*, 1192–1205.

Coudreuse, D.Y., Roël, G., Betist, M.C., Destrée, O., and Korswagen, H.C. (2006). Wnt gradient formation requires retromer function in Wnt-producing cells. Science *312*, 921–924.

Derijck, A.A., Van Erp, S., and Pasterkamp, R.J. (2010). Semaphorin signaling: molecular switches at the midline. Trends Cell Biol. *20*, 568–576.

Gao, C., and Chen, Y.G. (2010). Dishevelled: the hub of Wnt signaling. Cell. Signal. *22*, 717–727.

Gleason, J.E., Korswagen, H.C., and Eisenmann, D.M. (2002). Activation of Wnt signaling bypasses the requirement for RTK/Ras signaling during *C. elegans* vulval induction. Genes Dev. *16*, 1281–1290.

Green, J.L., Kuntz, S.G., and Sternberg, P.W. (2008). Ror receptor tyrosine kinases: orphans no more. Trends Cell Biol. *18*, 536–544.

Harris, J., Honigberg, L., Robinson, N., and Kenyon, C. (1996). Neuronal cell migration in *C. elegans*: regulation of Hox gene expression and cell position. Development *122*, 3117–3131.

Harterink, M., Kim, D.H., Middelkoop, T.C., Doan, T.D., van Oudenaarden, A., and Korswagen, H.C. (2011). Neuroblast migration along the anteroposterior axis of *C. elegans* is controlled by opposing gradients of Wnts and a secreted Frizzled-related protein. Development *138*, 2915–2924.

Hedgecock, E.M., Culotti, J.G., Hall, D.H., and Stern, B.D. (1987). Genetics of cell and axon migrations in *Caenorhabditis elegans*. Development *100*, 365–382.

Ji, N., Middelkoop, T.C., Mentink, R.A., Betist, M.C., Tonegawa, S., Mooijman, D., Korswagen, H.C., and van Oudenaarden, A. (2013). Feedback control of gene expression variability in the *Caenorhabditis elegans* Wnt pathway. Cell *155*, 869–880.

Kim, C., and Forrester, W.C. (2003). Functional analysis of the domains of the C elegans Ror receptor tyrosine kinase CAM-1. Dev. Biol. *264*, 376–390.

Kim, S., Ren, X.C., Fox, E., and Wadsworth, W.G. (1999). SDQR migrations in *Caenorhabditis elegans* are controlled by multiple guidance cues and changing responses to netrin UNC-6. Development *126*, 3881–3890.

Kim, E., Sun, L., Gabel, C.V., and Fang-Yen, C. (2013). Long-term imaging of *Caenorhabditis elegans* using nanoparticle-mediated immobilization. PLoS ONE *8*, e53419.

Korswagen, H.C., Herman, M.A., and Clevers, H.C. (2000). Distinct β-catenins mediate adhesion and signalling functions in *C. elegans*. Nature *406*, 527–532.

Korswagen, H.C., Coudreuse, D.Y., Betist, M.C., van de Water, S., Zivkovic, D., and Clevers, H.C. (2002). The Axin-like protein PRY-1 is a negative regulator of a canonical Wnt pathway in *C. elegans*. Genes Dev. *16*, 1291–1302.

Liu, Y., Shi, J., Lu, C.C., Wang, Z.B., Lyuksyutova, A.I., Song, X.J., and Zou, Y. (2005). Ryk-mediated Wnt repulsion regulates posterior-directed growth of corticospinal tract. Nat. Neurosci. *8*, 1151–1159.

Lyuksyutova, A.I., Lu, C.C., Milanesio, N., King, L.A., Guo, N., Wang, Y., Nathans, J., Tessier-Lavigne, M., and Zou, Y. (2003). Anterior-posterior guidance of commissural axons by Wnt-frizzled signaling. Science *302*, 1984–1988.

Maloof, J.N., Whangbo, J., Harris, J.M., Jongeward, G.D., and Kenyon, C. (1999). A Wnt signaling pathway controls hox gene expression and neuroblast migration in *C. elegans*. Development *126*, 37–49.

Masuda, H., Nakamura, K., Takata, N., Itoh, B., Hirose, T., Moribe, H., Mekada, E., and Okada, M. (2012). MIG-13 controls anteroposterior cell migration by interacting with UNC-71/ADM-1 and SRC-1 in *Caenorhabditis elegans*. FEBS Lett. *586*, 740–746.

Middelkoop, T.C., Williams, L., Yang, P.T., Luchtenberg, J., Betist, M.C., Ji, N., van Oudenaarden, A., Kenyon, C., and Korswagen, H.C. (2012). The thrombospondin repeat containing protein MIG-21 controls a left-right asymmetric Wnt signaling response in migrating *C. elegans* neuroblasts. Dev. Biol. *361*, 338–348.

Nishita, M., Enomoto, M., Yamagata, K., and Minami, Y. (2010). Cell/tissue-tropic functions of Wnt5a signaling in normal and cancer cells. Trends Cell Biol. *20*, 346–354.

Nomachi, A., Nishita, M., Inaba, D., Enomoto, M., Hamasaki, M., and Minami, Y. (2008). Receptor tyrosine kinase Ror2 mediates Wnt5a-induced polarized cell migration by activating c-Jun N-terminal kinase via actin-binding protein filamin A. J. Biol. Chem. *283*, 27973–27981.

Okkema, P.G., and Fire, A. (1994). The *Caenorhabditis elegans* NK-2 class homeoprotein CEH-22 is involved in combinatorial activation of gene expression in pharyngeal muscle. Development *120*, 2175–2186.

Ou, G., and Vale, R.D. (2009). Molecular signatures of cell migration in *C. elegans* Q neuroblasts. J. Cell Biol. *185*, 77–85.

Pan, C.L., Howell, J.E., Clark, S.G., Hilliard, M., Cordes, S., Bargmann, C.I., and Garriga, G. (2006). Multiple Wnts and frizzled receptors regulate anteriorly directed cell and growth cone migrations in *Caenorhabditis elegans*. Dev. Cell *10*, 367–377.

Polleux, F., Ince-Dunn, G., and Ghosh, A. (2007). Transcriptional regulation of vertebrate axon guidance and synapse formation. Nat. Rev. Neurosci. *8*, 331–340.

Salser, S.J., and Kenyon, C. (1992). Activation of a *C. elegans* Antennapedia homologue in migrating cells controls their direction of migration. Nature *355*, 255–258.

Sawa, H., and Korswagen, H.C. (2013). Wnt Signaling in *C. elegans*. (WormBook), http://www.ncbi.nlm.nih.gov/books/NBK19669/.

Schambony, A., and Wedlich, D. (2007). Wnt-5A/Ror2 regulate expression of XPAPC through an alternative noncanonical signaling pathway. Dev. Cell *12*, 779–792.

Su, M., Merz, D.C., Killeen, M.T., Zhou, Y., Zheng, H., Kramer, J.M., Hedgecock, E.M., and Culotti, J.G. (2000). Regulation of the UNC-5 netrin receptor initiates the first reorientation of migrating distal tip cells in *Caenorhabditis elegans*. Development *127*, 585–594.

Sulston, J.E., and Horvitz, H.R. (1977). Post-embryonic cell lineages of the nematode, *Caenorhabditis elegans*. Dev. Biol. *56*, 110–156.

Sym, M., Robinson, N., and Kenyon, C. (1999). MIG-13 positions migrating cells along the anteroposterior body axis of *C. elegans*. Cell *98*, 25–36.

Thorpe, C.J., Schlesinger, A., Carter, J.C., and Bowerman, B. (1997). Wnt signaling polarizes an early *C. elegans* blastomere to distinguish endoderm from mesoderm. Cell *90*, 695–705.

Wallingford, J.B. (2012). Planar cell polarity and the developmental control of cell behavior in vertebrate embryos. Annu. Rev. Cell Dev. Biol. *28*, 627–653.

Wang, X., Zhou, F., Lv, S., Yi, P., Zhu, Z., Yang, Y., Feng, G., Li, W., and Ou, G. (2013). Transmembrane protein MIG-13 links the Wnt signaling and Hox genes to the cell polarity in neuronal migration. Proc. Natl. Acad. Sci. U S A *110*, 11175–11180.

Whangbo, J., and Kenyon, C. (1999). A Wnt signaling system that specifies two patterns of cell migration in *C. elegans*. Mol. Cell *4*, 851–858.

Winston, W.M., Molodowitch, C., and Hunter, C.P. (2002). Systemic RNAi in *C. elegans* requires the putative transmembrane protein SID-1. Science *295*, 2456–2459.

Witze, E.S., Litman, E.S., Argast, G.M., Moon, R.T., and Ahn, N.G. (2008). Wnt5a control of cell polarity and directional movement by polarized redistribution of adhesion receptors. Science *320*, 365–369.

Wu, J., Duggan, A., and Chalfie, M. (2001). Inhibition of touch cell fate by *egl-44* and *egl-46* in *C. elegans*. Genes Dev. *15*, 789–802.

Zinovyeva, A.Y., and Forrester, W.C. (2005). The *C. elegans* Frizzled CFZ-2 is required for cell migration and interacts with multiple Wnt signaling pathways. Dev. Biol. *285*, 447–461.

Zinovyeva, A.Y., Yamamoto, Y., Sawa, H., and Forrester, W.C. (2008). Complex network of Wnt signaling regulates neuronal migrations during *Caenorhabditis elegans* development. Genetics *179*, 1357–1371.

Zou, Y., and Lyuksyutova, A.I. (2007). Morphogens as conserved axon guidance cues. Curr. Opin. Neurobiol. *17*, 22–28.